DNS STUDY OF MACH NUMBER EFFECTS ON TEMPORAL COMPRESSIBLE MIXING LAYER

Renaud Sauvage and Azeddine Kourta
Institut de Mécanique des Fluides de Toulouse
av Pr Camille Soula,
31400 Toulouse FRANCE

ABSTRACT

Direct numerical simulation on temporal compressible mixing layer are investigated for two convective Mach numbers namely 0.4 and 0.8. We discuss the compressibility effects on the main flow and also, on the fluctuating motion by statistical treatment.

1 INTRODUCTION

Fundamental research in the compressible turbulence field has been stimulated by a renewed interest in high-speed flows from aircraft industry. The development of propulsion systems based on supersonic combustion needs a better physical understanding of the compressible mixing layer. Study and understanding of the stability characteristics and transition to turbulence is of high theoretical and practical interest. The compressible mixing layer is a basic flow where mixing between two streams plays a predominant role for the aero-engine efficiency.

It is now well established that compressibility can directly influence the performance of supersonic combustion chamber. There are many experimental evidences of compressibility effects in mixing layers. The reduced growth of turbulent shear layer with increasing Mach number is one of the primary effects. This global effect has been observed by many authors [Papamoschou & Roshko(1988)] [Elliott & Samimy(1990)] [Papamoschou(1989)], but no convincing explanation has been given. This growth rate reduction causes the stabilization of the flow in supersonic regime [Sarkar(1995)]. Also, it was also observed [Clemens & Mungal(1992)] that the large-scale organised structures play a different role as Mach number increases. The roll-up and the pairing mechanisms exhibit similar features to the incompressible case if the Mach number is low whereas the scenario is quite different at higher Mach numbers (M_c)0.6). A review of compressible effect was discussed by [Lele(1994)].

To characterize the compressibility effects a convective Mach number M_c has been introduced by [Papamoschou & Roshko(1988)] based on previous work of Bogdanoff [Bogdanoff(1983)]. Recent experiments [Clemens & Mungal(1995)] revealed changes in turbulence statistics and typical eddy structure which becomes strongly three dimensional for convective Mach number greater than 0.6.

The linear stability analysis has also been developed [Ragab & Wu(1989)] [Sandham & Reynolds(1990)]. Temporal and spatial stability problems have been solved and have shown that the most amplified disturbances remain two dimensional for convective Mach number up to 0.6. Several direct numerical simulation [Sandham & Reynolds(1991)] [Luo & Sandham(1994)] [Vreman *et al.*(1996)] have been investigated for different convective Mach numbers in two and three dimensional cases. Mixing transition to small-scale turbulence and the different stages of vortex formations have been analyzed at low Reynolds number (between 50 and 600). Direct numerical simulation provides insight and guidance for the development of turbulence models notwithstanding the low Reynolds number limitations. Compressible existing models [Zeman(1991)] [Lejeune(1996)] don't correctly describe physics of turbulence anisotropy and three dimensional effects in high Mach number unsteady flows, typical characteristics of the compressibility. Solving all the relevant scales of motion contribute to the funda-

mental understanding of the transition to turbulence mechanisms in compressible shear layers.

In this study, our mean aim is to investigate mixing layer as real a mixing layer as possible to closely simulate and describe experimentally observed compressibility effects. Because of the high demand on computational resources for a three dimensional spatially growing mixing layer simulation, the temporal mixing layer is considered, which qualitatively exhibits the same physical phenomena as the spatial case. Two convective Mach numbers 0.4 and 0.8 are investigated. Initialized by the most amplified modes, pairing process occurs and the above-mentioned main caracteristics of compressibility appear. We rely our study on global variables, vizualisations and statistical treatment to reveal the compressible effects on the turbulence of the flow.

2 NUMERICAL METHODOLOGY

Three dimensional, time-dependent compressible Navier-Stokes equations have been solved by a finite volume method. The numerical technique uses a second order time and space accurate Mac Cormack explicit scheme. Based on the Simple Program Multiple Data method, the code uses Parallel Virtual Machine message passing library. Thus, the physical domain is split in sub-domains, each one being associated with one processor. The current simulations have been performed on a T3E massively parallel computer with 64 nodes. Typical two dimensional tests have validated the temporal code. Results of transitional mixing layer initialized by random disturbances have been compared with those of [Sandham & Reynolds(1991)] and shown good agreement. This is reported in [Sauvage & Kourta(1998)].

In order to reproduce a mixing layer as accurately as possible, non-reflecting characteristic boundary conditions developed by [Thompson(1987)] and modified by [Poinsot & Lele(1992)] for viscous flow are imposed at the normal boundaries (y). Streamwise (x) and spanwise (z) boundary conditions are treated as periodic. Uniform Cartesian grid is used in spanwise and streamwise directions whereas a refined mesh in the center of the layer is built with a sinus hyperbolic law. Two convective Mach numbers M_c 0.4 and 0.8 have been chosen to compare the compressibility behaviour which would be present in the mixing layer. M_c is defined as $M_c = (U_1 - U_2)/(c_1 + c_2)$ where U_1 and U_2 are the free-stream velocities and c_1 and c_2 are the corresponding sound speeds. Thus, the temporally evolving shear layer simulations are initialized with an hyperbolic tangent mean streamwise velocity profile and zero mean transverse and spanwise velocities. The temperature profile follows the Busemann-Crocco law assuming equality of the mean temperature in the two streams. All thermodynamic properties are initialized to uniform values. The initial Reynolds number is based on the velocity difference across the layer and the initial vorticity thickness. The vorticity thickness is defined as $\delta_\omega = (U_1 - U_2)/|d\overline{u}/dy|_{max}$. The initial flow field is superimposed with two and three dimensional perturbation modes obtained from linear stability analysis. We have developed a code solving the inviscid compressible equation of linear stability to calculate amplified modes and their associated eighenfunctions $\widehat{\Phi}$. Results were validated through comparison with various works [Sandham & Reynolds(1991)] [Lessen *et al.*(1965)]. The streamwise and the spanwise fundamental wavelengths (λ_x and λ_z) of the simulation are chosen to be the most instable wavelengths from linear stability theory. The streamwise and spanwise associated wavenumbers (k_x and k_z) are introduced by $k_x = 2\pi/\lambda_x$and $k_z = 2\pi/\lambda_x$. To specify the initial conditions, we define a single mode as $(\alpha, \beta) = (\frac{k_x \lambda_x}{2\pi}, \frac{k_z \lambda_z}{2\pi})$ where (αflβ) are the integer wavenumbers. Hence, for the 0.4 Mach number case, two dimensional perturbations are defined by (4,0), (2,0) and (1,0), the most amplified mode and its subharmonics, respectively. Even if the linear stability theory implies that the two-dimensional instability is the most amplified disturbance for $M_c < 0.6$, three dimensional perturbations are introduced by equal and opposite oblique modes (4,4), (4,-4), (2,2), (2,-2), (1,1), (1,-1). The amplitudes of perturbations have been chosen as 0.05 and 0.025 for the fundamental and subharmonic modes respectively. For $M_c = 0.8$ where the primary instability is three-dimensional, so two pair of equal and oblique modes (2,-2), (1,-1) were introduced. The instability amplitudes are chosen equal to 0.05. Numerical details on most amplified mode and computational box lenght are summarised below.

M_c	L_x	L_y	L_z	k_x	θ	Rey
0,4	30,70	30	30,70	0,818	45°	200
0,8	24,51	30	27,49	0,512	41,72°	400

The angle of the disturbance is defined by $\tan\theta = k_z/k_x$. The mesh size uses a 192 × 192 × 192 grid. This mesh is fine enough to compute all relevent scales. 50 T3E massively parallel computer hours have been needed to simulate 8 and 3 wavelenghts for the 0,4 and 0,8 cases respectively.

3 RESULTS

So as to describe the compressibility effects in subsonic flows, two convective Mach numbers have been chosen namely 0,4 and 0,8. During the simulation, the one dimensional streamwise energy spectrum $E(k_x)$ (figure1) has been computed to ensure adequate resolution. It was defined by $E(k_x) = \iint \widetilde{u}_i(k_x)\,\widetilde{u}_i^{\dagger}(k_x)\,dydz$ where †indicates a complex conjugate. Same definition was used for the spanwise component. As the wavenumber increases, a higher fall in energy occurs. The energy transfert from the large scales to the small ones is well established. The temporal development of the vorticity and momentum thicknesses is shown in figure 2. The evolution of these quantities is correlated to pairing mechanism. For the 0.4 convective Mach number, at the beginning, the shear layer extends by diffusion. When the most amplified modes are satu-

rated, four spanwise well-developed vortices come together bound by braid regions at t=20.07 shown in the figure 4a). The now familiar pairing could henceforth begin to process. The decrease of the momentum thickness after t=23.2 is due to the elliptical form of the two resulting eddies (fig. 4b). Spiral arms of weaker spanwise vorticity are ejected away from the paired structures. The second pairing could begin (fig. 4c). As the vorticity thickness increases during the simulation, the Reynolds number also increases with time and reaches 1680. This pairing process is two dimensional and no three dimensional instabilities of the structure appear. The initial three dimensional perturbations have not been sufficiently amplified to destabilize the spanwise direction. Several simulations have been investigated on the influence of initial mode amplitudes. The behaviour of the eddies didn't change.

For $M_c = 0.8$, only the first step of the evolution of the mixing layer is plotted to compare with the previous case. The compressibility effect is clear from this curve. The growth rate defined by $d\delta_\theta/dt$ is reduced as M_c increases. Another important effect of the compressibility is the three dimensional behaviour of the flow at 0.8. In figure 5, vizualisations depict three dimensional vorticity isosurfaces and cut xz vorticity plane in the middle of the shear layer. When the most amplified modes achieve saturation , two vortices appear in the xy plane which develop Λ-shaped structures in the spanwise direction. The "hair-pin" mechanism can occur in both the upper- and lower-stream flows.

Mixing layer self-similarity requires [Moser & Rogers(1993)] linear evolution of the momentum thickness. Since the computational domain is finite in the homogeneous directions, it is very difficult to achieve self-similarity with direct numerical simulation initialized by small disturbances. Nevertheless, the growth rate can be approximated on the figure 2 when pairing can no longer occur at the end of the simulations, giving 0.112 and 0.053 at Mc=0.4 and 0.8 respectively. We have plotted these values (see figure 3), normalised by the incompressible growth rate $d\delta/dt = 0.181$, given by [Brown & Roshko(1974)] to compare with experimental data gathered by [Lele(1994)]. The result is in good agreement with the self-similarity hypothesis.

Now we will analyse the fluctuating motion. We introduce statistical profiles at the end of the simulations, when a single vortex subsists and cannot undergo an other pairing. Averaged variables in a temporal mixing layer are function of time and the normal coordinate y only. They are obtained by averaging all the variables in the homogeneous plane (x,y). formed by steamwise and spanwise directions. Whereas [Vreman *et al.*(1996)] used integrated profiles, we purpose here to study balances of Reynolds stress, energy and vorticity equations in order to describe locally the compressibility behaviour in the shear layer.The Reynolds stress averaged equations using weighted mass average are:

$\frac{d}{dt}(\widetilde{\rho u_i'' u_j''}) = \Pi_{ij} + \Phi_{ij} + \varepsilon_{ij} + T_{ij} + \Psi_{ij} + D_{ij} + \Upsilon_{ij}$

with $\Pi_{ij} = -\widetilde{\rho u_i'' u_k''}\widetilde{U_{j,k}} - \widetilde{\rho u_j'' u_k''}\widetilde{U_{i,k}}$ = production

$\Phi_{ij} = -\left(\widetilde{\rho u_i'' u_j'' u_k''}\right)_{,k}$ = turbulent diffusion

$\varepsilon_{ij} = -\overline{\sigma_{ik}' \frac{\partial u_j''}{\partial x_k}} - \overline{\sigma_{jk}' \frac{\partial u_i''}{\partial x_k}}$ = viscous dissipation

$T_{ij} = -\widetilde{u_i''}\left(\overline{P}_{,j} - \overline{\sigma_{jk}}_{,k}\right) - \widetilde{u_j''}\left(\overline{P}_{,i} - \overline{\sigma_{ik}}_{,k}\right)$ = turbulent mass flux

$\Psi_{ij} = \left(\overline{\sigma_{ik}' u_j''}\right)_{,k} + \left(\overline{\sigma_{jk}' u_i''}\right)_{,k}$ = molecular diffusion

$D_{ij} = -\left(\overline{p' u_i''}\right)_{,j} - \left(\overline{p' u_j''}\right)_{,i}$ = pressure gradient

$\Upsilon_{ij} = \overline{p'\left(u_{i,j}'' + u_{j,i}''\right)}$ = pressure-srain

Reynolds stress balances reveal that the contributions of $\widetilde{\rho u_1'' u_3''}$ and $\widetilde{\rho u_2'' u_3''}$ are negligible compared to other components for the two cases, their amplitude is 5 % of the smallest diagonal component . Furthermore, (3,3) is also negligible for 0.4 case as explained above. The normal profiles for the tensor Π_{ij}, Φ_{ij}, D_{ij} and Υ_{ij} have been plotted in figure 6 for Mach number 0.4, nondimentionalized by $\rho_{\inf} U_{\inf}^3/\delta_{\omega_0}$. The production term Π_{12} is negative, while Π_{11} is positive. The other componants are negligible. All along the normal direction, the amplitude of Π_{12} is higher than in the streamwise direction. Thus, the Reynolds stress R_{12} supplies mean motion with energy through the production term whereas the streamwise component Π_{11} takes this energy back. This energy is later redistributed by others terms and supplied to the fluctuating motion. The pressure strains Υ_{11} and Υ_{22} seem to be stricktly opposite whereas Υ_{12} is negative. The pressure strain acts to distribute energy between streamwise and normal directions. Compared to the other terms, the dissipation has little contribution to the shear layer development. Futhermore, the turbulent diffusion Φ_{ij} plays the role of energy well and contribute to propagate turbulence into the layer. In the Reynolds averaged equations, only D_{22} and D_{12} play significant parts in the energy balance. D_{12} balances the important turbulent diffusion Φ_{12} whereas the less energetic D_{22} component contributes to balance the pressure-strain influence.

The reduction of the growth rate of the mixing layer for 0.8 case is clearly shown with the normal profile of the Reynolds averaged stress (figure 7). Stress amplitudes are lower than $M_c = 0.4$ case. Symmetric behaviour in the normal profile is explained by the transitional process which has not hitten the shear layer. This explanation is supported by the low rate of the normal Reynolds stress componant and also, by the higher streamwise production amplitude in relation to R_{11}, R_{33} and R_{12}. Here, Π_{22}, Π_{33} and Π_{12} which are negative, contribute with different intensities to keep mean motion going on Π_{11} component. The pressure strains' contribution to energy balance is as important as in 0.4 case. However, the streamwise component Υ_{11} which is also negative, distributes energy not only to normal direction but also to the spanwise direction with equal intensity. In other words, tridimensional-

ity and mixing layer growth are both supported by the streamwise fluctutating flow.

4 CONCLUSION

A study of compressible effects on large structures has been described in this paper. DNS of temporal compressible mixing layer have been performed for two convective Mach numbers 0.4 and 0.8, using second order Mac Cormack scheme and parallel algorithm. Initially perturbated by the most amplified modes of linear stability theory, the shear layer grows while giving birth to large eddies, which roll up and pair successively according to the Kelvin-Helmoltz process. As the convective Mach number increases, the growth rate of the mixing layer decreases as predicted by linear stability theory and experiments by a factor of two. Whereas the flow is dominantly two-dimensional for the $M_c = 0.4$ case, three-dimensionality is characterized by Λ-shaped vortex development for $M_c = 0.8$ case in the transitional process. This behaviour is explained by the greater importance of the spanwise Reynolds stress components in the latter case and the lower contribution of the Reynolds stress components.

Acknowledgments

This work was performed at Institut de Mécanique des Fluides de Toulouse. Computational support provided by IDRIS at Orsay (France)is gratefully acknowledged.

References

[Bogdanoff(1983)] BOGDANOFF, D. 1983 Compressibility effects in turbulent shear layers. *AIAA Journal* **21**, 926–927.

[Brown & Roshko(1974)] BROWN, G. L. & ROSHKO, A. 1974 On density effects and large scale structure in turbulent mixing layers. *J. Fluid Mech.* **64**, 775–816.

[Clemens & Mungal(1992)] CLEMENS, N. & MUNGAL, M. G. 1992 Two- and three-dimensional effects in the supersonic mixing layer. *AIAA Journal* **30**, 973–981.

[Clemens & Mungal(1995)] CLEMENS, N. & MUNGAL, M. G. 1995 Large-scale structure and entrainment in the supersonic mixing layer. *J. Fluid Mech.* **284**, 171–216.

[Elliott & Samimy(1990)] ELLIOTT, G. S. & SAMIMY, M. 1990 Compressibility effects in free shear layers. *Phys. Fluids* **A** (2), 1231–1240.

[Lejeune(1996)] LEJEUNE, C., K. A. 1996 Modelling of high speed turbulent flows. *AIAA Paper* **96-2041**.

[Lele(1994)] LELE, S. K. 1994 Compressibility effects on turbulence. *Ann. Rev. Fluid Mech.* **26**, 211–254.

[Lessen *et al.*(1965)] LESSEN, M., FOX, J. & ZIEN, H. 1965 Compressible mixing layer growth rate and turbulence characteristics. *J. Fluid Mech.* **23**, 355–367.

[Luo & Sandham(1994)] LUO, K. H. & SANDHAM, N. D. 1994 *On the Formation of Small Scales in a Compressible Mixing Layer*. Kluwer.

[Moser & Rogers(1993)] MOSER, R. D. & ROGERS, M. 1993 The three-dimensional evolution of a plane mixing layer: Pairing and transition to turbulence. *J. Fluid Mech.* **247**, 275–320.

[Papamoschou(1989)] PAPAMOSCHOU, D. 1989 Structure of the compressible turbulent shear layer. *AIAA Paper* **89-0126.**

[Papamoschou & Roshko(1988)] PAPAMOSCHOU, D. & ROSHKO, A. 1988 The compressible turbulent mixing layer: An experimental study. *J. Fluid Mech.* **197**, 453–477.

[Poinsot & Lele(1992)] POINSOT, T. J. & LELE, S. K. 1992 Boundary conditions for direct simulations of compressible viscous reacting flows. *J. Comp. Physics* **101**, 104–129.

[Ragab & Wu(1989)] RAGAB, A. & WU, J. L. 1989 Linear instabilities in two-dimensional compressible mixing layers. *Phys. Fluids* **A** (6), 957–966.

[Sandham & Reynolds(1990)] SANDHAM, N. D. & REYNOLDS, W. C. 1990 Compressible mixing layer: Linear theory and direct simulation. *AIAA Journal* **28**, 618–624.

[Sandham & Reynolds(1991)] SANDHAM, N. D. & REYNOLDS, W. C. 1991 Three-dimensional simulations of large eddies in the compressible mixing layer. *J. Fluid Mech.* **224**, 133–158.

[Sarkar(1995)] SARKAR, S. 1995 The stabilizing effect of compressibility in turbulent shear flow. *J. Fluid Mech.* **282**, 163–186.

[Sauvage & Kourta(1998)] SAUVAGE, R. & KOURTA, A. 1998 Compressible effects on temporal direct numerical simulation. *Third International Workshop on Vortex Flows and Related Numerical Methods* .

[Thompson(1987)] THOMPSON, K. W. 1987 Time dependent boundary conditions for hyperbolic systems. *J. Comp. Phys.* **68**, 1–24.

[Vreman *et al.*(1996)] VREMAN, A. W., SANDHAM, N. D. & LUO, K. H. 1996 Compressible mixing layer growth rate and turbulence characteristics. *J. Fluid Mech.* **320**, 235–258.

[Zeman(1991)] ZEMAN, O. 1991 On the decay of compressible isotropic turbulence. *Phys. Fluids* **A** (3), 951–955.

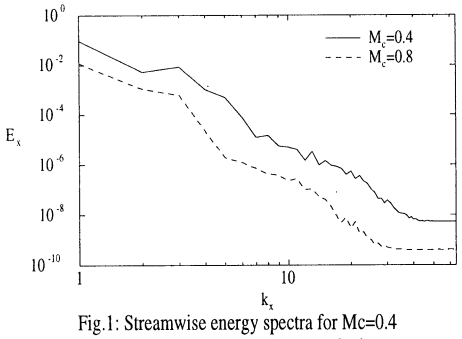

Fig.1: Streamwise energy spectra for Mc=0.4 and 0.8 at t=23.05 and 25.2 respectively

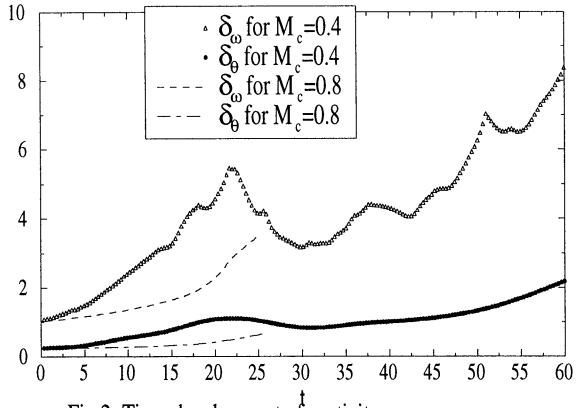

Fig.2: Time-development of vorticity and momentum thicknesses.

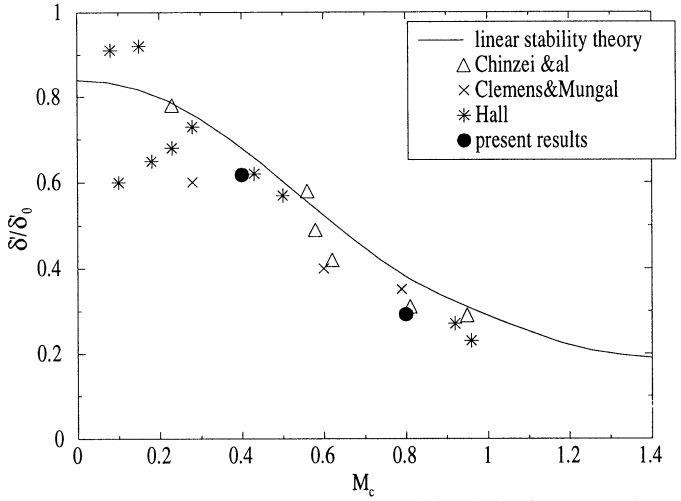

Fig.3: Comparaison of normalised compressible mixing layer growth rates

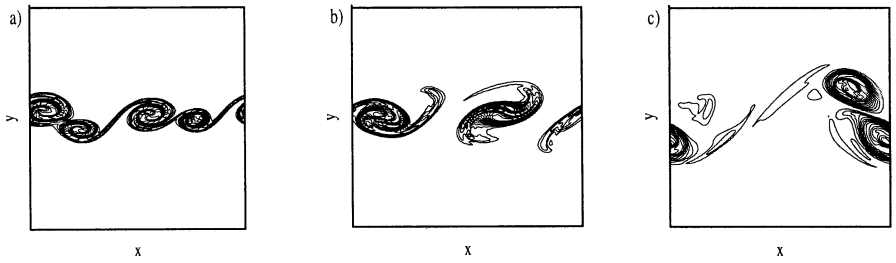

Fig.4: Vorticity contours in the plane z=Lz/2, at t= a) 13.50, b) 30.48 and c) 59.29.

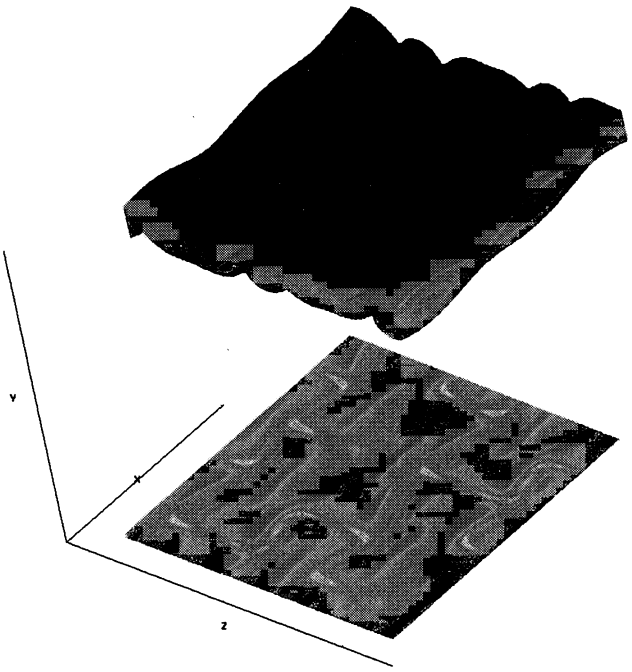

Fig.4: Layer of vorticity isosurfaces for Mc=0.8 at t=21.2. Below, y=0 vorticity plane.

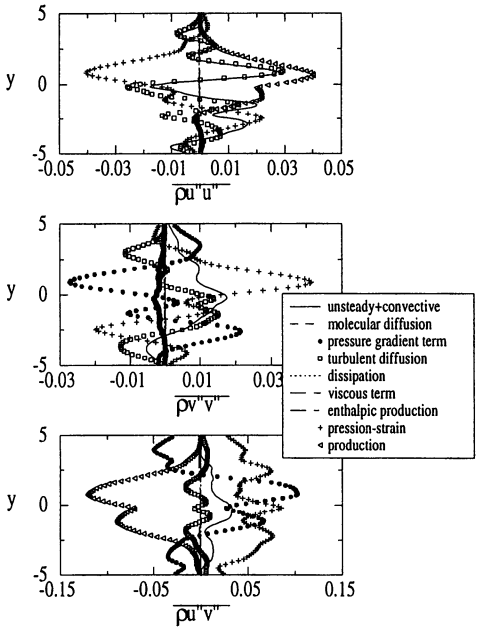

Fig.6: Reynolds stress balance for Mc=0.4 at t=20.07

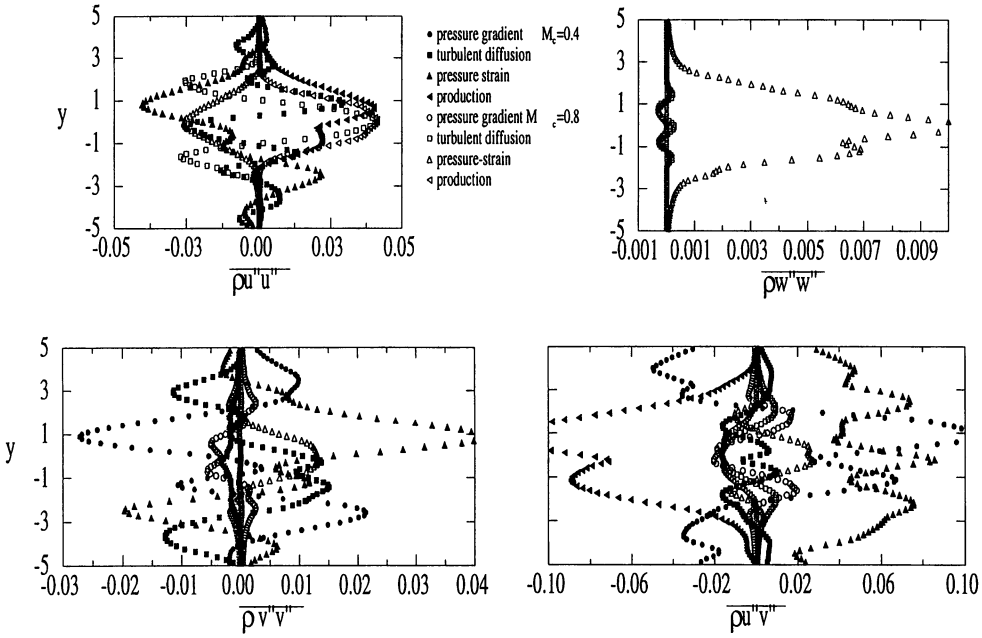

Fig.7: Production, pressure-strain, turbulent diffusion and pressure gradient components comparaison for the Mc=0.4 (hollowed symbols) and 0.8 (filled symbols). Values for 0.8 case were multiplied by 5 for a better visibility.